

Research article

# Rotational molding of LLDPE/coir fiber composites: Effect of fiber on mechanical, thermal, morphological and flammability properties

Lumirca Del Valle Espinoza León<sup>1</sup>, Viviane Alves Escócio<sup>1</sup>, Leila Lea Yuan Visconte<sup>1,2</sup>, Ana Maria Furtado de Sousa<sup>3</sup>, Ana Lúcia Nazareth da Silva<sup>1,2</sup>, Elen Beatriz Acordi Vasques Pacheco<sup>1,2\*</sup>

<sup>1</sup>Instituto de Macromoléculas Professora Eloisa Mano/Programa em Ciência e Tecnologia de Polímeros, Universidade Federal do Rio de Janeiro, 2030 Horácio Macedo Avenue, Technology Center, block J, 21941-598, Brazil

<sup>2</sup>Escola Politécnica/Programa de Engenharia Ambiental, Universidade Federal do Rio de Janeiro, 149 Athos da Silveira Ramos Avenue, Technology Center, block A, 21941-909, Ilha do Fundão, Rio de Janeiro, Brazil

<sup>3</sup>Instituto de Química, Universidade do Estado do Rio de Janeiro, 524 São Francisco Xavier Street, Pavilhão Haroldo Lisboa da Cunha, 310, Maracanã, 20550-900, Rio de Janeiro, RJ, Brazil

Received 18 September 2024; accepted in revised form 15 October 2024

**Abstract.** This study uses a rotomolding procedure to produce hollow cubes made of linear low-density polyethylene (LLDPE) and coconut fibers (CF). The purpose is to investigate the effect of different CF content (0, 5, 12.5, and 20 wt%) and size (100 and 50 mesh) on composite properties. As the CF content rises, the density of all composites decreases due to an increase in material porosity, a result of poor adhesion between the fiber and LLDPE. Impact strength reduced as the content of CF increased, except for the composite with 5 wt% of CF and 50 mesh size. The ineffective adhesion between coir fibers and LLDPE, along with the presence of voids in the matrix, caused the mechanical properties to deteriorate as the CF content increased. The flammability test revealed that all samples dripped. The neat LLDPE sample deformed, whereas the LLDPE/CF composites maintained their shape. This behavior suggests that CF plays a structural role in burning composites. Maleic anhydride-grafted polyethylene (MAPE), calcium stearate, and magnesium stearate additives did not contribute to reducing the composite's porosity. MAPE was the only additive that did not reduce the elastic modulus of composites.

**Keywords:** rotational molding, linear low-density polyethylene, coconut fibers, recycling, composites

## 1. Introduction

The rotational molding (or rotomolding) process uses primarily thermoplastic materials to produce large hollow parts with low residual stress levels. It has a longer cycle time than extrusion or injection molding; therefore, it is important to choose polymers with high thermal stability. Linear low-density polyethylene (LLDPE) is the most frequently utilized material for rotomolding, as it demonstrates resistance to thermal degradation over extended durations [1–6].

Natural fibers have an eco-friendly nature and are sustainable and renewable [7–9]. The use of lignocellulosic fibers, especially their residues, in polymeric composites is environmentally beneficial because it preserves natural resources, reduces waste, and can enter the production cycle while meeting the principles of the circular economy [10].

The sustainability of natural fiber composites is examined based on life cycle assessment (LCA), a methodology formulated to investigate the potential environmental impact of products at all stages of

\*Corresponding author, e-mail: [elen@ima.ufrj.br](mailto:elen@ima.ufrj.br)

© BME-PT

their life cycle [11–13]. The LCA shows that using natural fibers instead of synthetic fibers is environmentally more sustainable. For example, sisal fiber has much lower greenhouse gas emissions (75–95%) and non-renewable energy use (85–95%) compared to glass fiber [14]. It is worth mentioning that environmental impact values of natural fibers are dependent on the plantation location and production practices [13, 14].

Producing polymeric composites with lignocellulosic fibers through rotational molding is a challenge that requires overcoming obstacles, such as achieving a more homogenous mixture of polymer and lignocellulosic fibers. Therefore, the scientific community is driven to find solutions to produce high-quality thin-walled products, which in turn motivates the development of further studies [2, 15–18].

By rotational molding, Gupta and Ramkumar [2] produced LLDPE composites containing 3, 5, 7, and 10 wt% of coir fibers. According to the authors, a lower fiber content was associated with improved fiber distribution and a robust filler-polymer interaction. In general, all composites displayed a slight increase in tensile strength and elastic modulus, with the exception of the composite with 10 wt% of fiber. Abhilash and Singaravelu [19] utilized rotational molding to produce composites with LLDPE and bamboo fibers at 5, 10, and 15 wt%. Before use, these lignocellulosic fibers underwent a 5% NaOH (mercerization) treatment. The authors do not recommend the addition of 15 wt% of bamboo to LLDPEs due to the occurrence of fiber agglomeration at the corners of the mold and the observation of poor fiber matrix bonding and adhesion. They also noted that composites containing 5 wt% of bamboo exhibited a superior balance compared to neat LLDPE. Although these two studies [2, 19] arrive at similar conclusions regarding the effect of fiber content on mechanical properties, they used lignocellulosic fibers of different sizes, namely coir fibers with an average particle size of 125  $\mu\text{m}$  [2] and chopped bamboo fibers with a maximum length of 5 mm [19]. In another study, Andrzejewski *et al.* [16] produced composites based on LLDPE and poly(lactic acid) (PLA), both filled with buckwheat hull, using rotational molding. The purpose was to investigate the influence of the amount of filler (up to 30 wt%) and the particle size (50, 50–200, and 200–500  $\mu\text{m}$ ) on structure-property correlation. According to the authors, it was challenging to produce composites from

buckwheat hulls with particle sizes smaller than 50  $\mu\text{m}$ . Furthermore, the high porosity makes mechanical properties worse.

It is known that the interfacial bonding or adhesion between hydrophilic fibers and hydrophobic matrices affects mechanical properties [20], which maleating agents may improve [21]. A study by Robledo-Ortiz *et al.* [22] examined the use of maleic anhydride-grafted polyethylene (MAPE) as a surface treatment for agave and coir fibers to produce LLDPE composites with 20 and 30 wt% of fibers via rotational molding. According to the authors, pretreatment of the fibers with MAPE modified their surface chemistry and enhanced compatibility and adhesion with the polymer matrix. This result was supported by a comparison of composite properties with treated and untreated fibers. Cisneros-López *et al.* [23] studied the effect of agave, coir, and pine fiber contents (10, 20, 30, and 40 wt%) on the properties of polyethylene composites with untreated and MAPE-treated fibers. The authors stated that the surface treatment was more effective for agave and coir fibers because those fibers had higher holocellulose and lower extractive contents than pine fibers. Furthermore, the treatment improved fiber-matrix interface quality in terms of adhesion, wettability, and compatibility, resulting in better mechanical properties. In conclusion, there are few studies (Gupta and Ramkumar [2]; Robledo-Ortiz *et al.* [22]; Cisneros-López *et al.* [23]; Abhilash and Singaravelu [19]) that investigated the production of LLDPE/coir fiber composites by rotational molding, whose characterizations were carried out by thermal, mechanical, and morphological properties. This data supports that the rotational molding process does not receive as much attention as extrusion and injection for producing more sustainable composites.

Therefore, the purpose of this study is to provide more technical data about the LLDPE/coir composites processed by rotational molding, with the aim of contributing to the growth and advancement of scientific knowledge about this subject in the literature. Thin-walled hollow cubes with different sizes and amounts of fibers were made in this study using composites of LLDPE and coir fibers, with or without processing additives. All composites were characterized in terms of morphology, thermal and mechanical resistance, and water absorption properties. Furthermore, this study conducts the flammability test and thermogravimetric analysis to measure thermal

stability, two investigations not included in the previously cited papers. It was also evaluated how the presence of the additives calcium stearate (CaSt) and magnesium stearate (MgSt) interfered with the properties of the rotational-molded composites.

## 2. Experimental

### 2.1. Materials

Linear low-density polyethylene (LLDPE) ML3602U specified for rotational molding (melt temperature: 127 °C, density: 0.937 g·cm<sup>-3</sup>; melt flow index: 5 g·10 min<sup>-1</sup> at 190 °C, 2.16 kg<sup>-1</sup>) was supplied by the Braskem company. The LLDPE in the form of pellets was ground to a 40 mesh size using a Pallman PKMem micronizer.

Coir fiber waste (CF) was donated by *Projeto Coco Verde* Company in a chopped shape. The coir sample was then milled (Marconi, model Ma580) and classified into 100 mesh (coded as CF-100) (149 μm) and 50 mesh (coded as CF-50) (297 μm) (Tyler). The coir fiber was just mechanically pretreated because this study prioritized the development of processes that generate minimal effluents. The use of pretreatment of fibers with chemicals [24] generally produces effluents that cause negative impacts in production and that are added to the final product [25]. The lignin content of coconut fiber was determined in duplicate according to the Klason method (TAPPI T13M-54), whose value was 41.3±0.2%, and it is comparable to the values reported in the literature (31–46 wt%) [26–29]. α-Cellulose contents were determined in duplicate according to the TAPPI T19m-54 standard, adapted for lignocellulosic fibers [30], and its value was 52.0±8.5%. Literature [8, 31, 32] reports cellulose values between 27 and 44% for coconut fiber. The density of the coir was 1.60±0.10 g·cm<sup>-3</sup>, evaluated according to ASTM D792-08.

Maleic anhydride grafted polyethylene (MAPE) (0.4 wt% maleic anhydride, density 0.905 g·cm<sup>-3</sup>), calcium stearate (CaSt) (density 1.08 g·cm<sup>-3</sup>), and magnesium stearate (MgSt) (density 1.03 g·cm<sup>-3</sup>) were evaluated as additives. MAPE and CaSt were supplied by Sigma-Aldrich, and MgSt was donated by the Universidade do Estado do Rio de Janeiro. MAPE, received in pellet shape, was ground to 40 mesh size using a Pallman PKMem micronizer. CaSt and MgSt were in powder form and used as received. MAPE was chosen as a coupling agent for the LLDPE and coir fibers [3]. The carboxylated

**Table 1.** Lists the functions of the components in formulation.

Component	Function
Linear low-density polyethylene (LLDPE)	Matrix
Coir fiber waste (CF)	Renewable filler
Maleic anhydride grafted polyethylene (MAPE)	Assessment as compatibilizer additive
Calcium stearate (CaSt) and magnesium stearate (MgSt)	Assessment as compatibilizer additive and additive for avoid of pinholes formation [33]

salts CaSt and MgSt have a lower molecular weight compared to MAPE and are recognized as sintering enhancers for rotomolding polyethylene. They help to reduce the number of bubbles in the final product [33]. The purpose of testing those stearates is to determine their effectiveness as an additive for the rotomolding process, in comparison to MAPE. Kulikov *et al.* [33] reported that products with surfaces free of pinholes are made by adding 0.01 to 0.04 wt% of fatty acid salt to olefin polymer-based rotational molding mixtures. In this work, the amounts of CaSt and MgSt were set at 1 wt%, in order to minimize bubble formation caused by the presence of coir fiber. The MAPE amount was also fixed at 1 wt% to allow for better comparisons of properties. The mold release agent used was Mepcodesmold 4200<sup>®</sup>. Table 1 describes the function of each component in the composite formulation.

### 2.2. Composites preparation

Table 2 and Table 3 show, respectively, the formulations of the LLDPE/CF composites without and with the additives. The experimental code is X/Y/W/Z, where X and Y are the amounts of LLDPE and CF [wt%], W is the mesh of CF (CF-50 and CF-100), and Z is the type of additive (MAPE, CaSt, MgSt). The Z character appears only in the codes for composites containing additives.

**Table 2.** Formulations of LLDPE/CF composites with no additive [wt%].

LDPE/CF/CF-mesh	LLDPE	CF-50	CF-100
100/0/0	100	–	–
95/5/50	95	5	–
87.5/12.5/50	87.5	12.5	–
80/20/50	80	20	–
95/5/100	95	–	5
87.5/12.5/100	87.5	–	12.5
80/20/100	80	–	20

**Table 3.** Formulations of LLDPE/CF-100 composites with additive [wt%].

LDPE/CF/CF-mesh/additive	LLDPE	CF-100	MAPE	CaSt	MgSt
100/0/0/0	100	–	–	–	–
95/5/100/0	95	5	–	–	–
95/5/100/MAPE	94	5	1	–	–
95/5/100/CaSt	94	5	–	1	–
95/5/100/MgSt	94	5	–	–	1

The total amount of each formulation placed in the rotating molder (906 g) was determined according to Equation (1) [34, 35]:

$$Q_m = A_S \cdot E_P \cdot \rho_p \quad (1)$$

where  $Q_m$  is the amount of material [g],  $A_S$  the surface area of the mold cavity [cm<sup>2</sup>],  $E_P$  is the part thickness (0.3 cm),  $\rho_p$  the polymer material density [g·cm<sup>-3</sup>].

Firstly, all components were weighted and then dried separately in an oven at 60 °C for 24 h. Then, the components of each formulation (Table 1 and Table 2) were manually mixed for 5 min in a 3 l plastic container.

The composites were prepared in a Rotoline 0.50 LAB Rotational Molding Machine (Figure 1a). The mold release agent was applied inside the cubic iron mold (24×24×24 cm), and then the mixture of composite was added to the mold, which was attached to the small axis of the machine. The set-up parameters used were recirculation fan speed of 1300 rpm (manual of Rotoline); oven temperature of 250 °C [36, 37], axis rotation speed (large:small) of heating 4:1; axis rotation speed (large:small) cooling of 2:1 [36–38], cycle time heating of 15 min, and cycle time cooling of 15 min. This study uses a lower oven temperature for rotational molding of LLDPE composites with lignocellulosic fibers than those used in previous studies (260 °C [23], 280 °C [17], and 300 °C [2]). At the end of processing, the hollow cube was taken off from the mold. The test specimens were cut from cubes according to the ASTM standards to assess the morphology, mechanical and thermal properties, density, water absorption, melt flow index, and flammability, comparing the results with those of the neat LLDPE (code 100/0/0, Table 1 and Table 2). Figure 1 shows a photo of the Rotoline 0.50 LAB Rotational Molding Machine (Figure 1a) and samples of cubes made from different composites (Figure 1b).

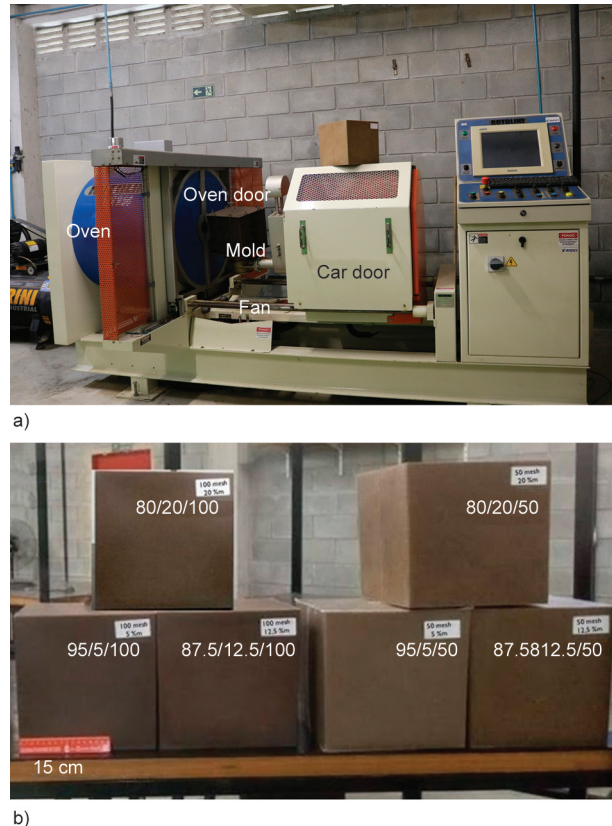


**Figure 1.** a) Rotoline 0.50 LAB Rotational Molding Machine and b) cubes produced with 95/5/50, 87.5/12.5/50, 80/20/50, 95/5/100, 87.5/12.5/100, and 80/20/100 composites. (The red rule measures 15 cm.)

## 2.3. Characterization

### 2.3.1. Morphological analysis by scanning electron microscopy

The CF-100 and CF-50 fiber samples, as well as the cryofractured surfaces of the composites, were examined using a JEOL JSM-6510LV scanning electron microscope (SEM) to evaluate their morphologies. The samples were carbon taped to metal support stubs and then gold-coated. The purpose of this analysis was to observe differences between CF-100 and CF-50 fiber morphologies, as well as the presence of bubbles and the adherence of fiber to matrix in the interphase of rotomolded composites.

### 2.3.2. Density of LLDPE and LLDPE/CF composites

The density was determined based on ASTM D792-20 and calculated using Equation (2). The test specimen with dimensions of 20×20×3 mm was weighed, suspended in air by a metal support, and then immersed in ethanol at 23 °C in a beaker. This analysis was done in duplicate.

$$\text{Density} = \frac{m_a}{m_a - m_b} \cdot \rho_{\text{ETOH}} \quad (2)$$

where  $m_a$  is the sample mass weighed in air;  $m_b$  is the sample mass weighed in ethanol;  $\rho_{\text{ETOH}}$  is the ethanol density at 23 °C (0.80 g·cm<sup>-3</sup>) [39].

The theoretical densities of LLDPE/CF composites were calculated using Equation (3), in which  $\rho_{\text{LLDPE}}$  and  $\rho_{\text{CF}}$  are, respectively, the experimental densities determined for neat LLDPE and CF, and  $w_{\text{LLDPE}}$  and  $w_{\text{CF}}$  are, respectively, the mass fraction of LLDPE and CF in the composite (Table 1 and Table 2).

$$\text{Theoretical density} = \rho_{\text{LLDPE}} \cdot w_{\text{LLDPE}} + \rho_{\text{CF}} \cdot w_{\text{CF}} \quad (3)$$

### 2.3.3. Melt flow index

The melt flow index (*MFI*) was measured at 2.16 kg and 190 °C using a Dynisco LMI-4003 melt indexer, based on the ASTM D1238-23a standard testing procedure. About 10 g of each composite were cut into 0.5×0.5 cm pieces using scissors. Prior to testing, all samples were dried in an air-circulated oven at 60 °C for 24 h. The *MFI* test result represents an average of five replicates.

### 2.3.4. Thermogravimetric analysis

Thermogravimetric analyses (TGA) were conducted on a Q500 series thermogravimetric analyzer from TA Instruments, according to ASTM E-1356-03. Samples (about 10 mg) were submitted to testing at a scanning temperature range of 25 to 700 °C and a heating rate of 10 °C·min<sup>-1</sup> in a nitrogen atmosphere with a flow rate of 20 ml·min<sup>-1</sup>.

### 2.3.5. Crystallinity degree measurement

A TA Instruments Q1000 differential scanning calorimeter (DSC) was used to evaluate the crystallinity degree of the neat LLDPE and their composites. The DSC tests were run under the following cycles: heating from 25 to 200 °C at a heating rate

of 10 °C·min<sup>-1</sup>, cooling to 25 °C at a cooling rate of 10 °C·min<sup>-1</sup>, and reheating from 25 to 200 °C at a heating rate of 10 °C·min<sup>-1</sup>. Analysis was conducted in N<sub>2</sub> with a sample mass ranging from 4 to 11 mg. The crystallinity of the samples was calculated according to Equation (4) [29, 40].

$$\chi_c [\%] = \frac{\Delta H_f}{\Delta H_f^0 \cdot w} \cdot 100 \quad (4)$$

where  $\chi_c$  is the crystallinity degree,  $\Delta H_f$  the variation in the melt enthalpy of the composite,  $\Delta H_f^0$  is the melting enthalpy of 100% crystalline PE (293 J·g<sup>-1</sup>) [41, 42] and  $w$  is the LLDPE mass fraction in the composites.

### 2.3.6. Water absorption

The water absorption test was performed based on the ASTM D570-22 standard. The test specimens with dimensions of 20×20×3 mm were completely immersed in distilled water at 25 °C. They were thereafter removed at the times of 15, 30, 45 min, 1, 1.5, 2 h, 1, 2, and 7 days. For each of those times, after the sample was removed, the water on the surface was wiped out with absorbent paper, and the sample was promptly weighed to the nearest 0.0001 g. The water absorption was quantified using Equation (5):

$$\begin{aligned} \text{Increase in weight} [\%] &= \\ &= \frac{\text{wet weight} - \text{initial weight}}{\text{initial weight}} \cdot 100\% \quad (5) \end{aligned}$$

### 2.3.7. Mechanical properties

Tensile properties were determined according to ASTM D638-22 using five test specimens (Type IV) and an EMIC Model DL3000 testing machine with a 5 kN load cell, a maximum grip displacement of 65 mm, and a crosshead speed of 5 mm/min. Flexural strength was measured according to ASTM D790-17. The test was conducted on an EMIC Model DL3000 testing machine. The test specimens were 127 mm long, 12 mm wide, and 3.2 mm thick. Span length was 52 mm for the three-point bending test. Five test specimens were used for each composition. Izod pendulum impact resistance was performed using a CEAST Resil Impactor tester with a 2.75 J pendulum at an angle of 150°, according to the ASTM D256-23e1 standard. The test specimens,

notched in accordance with the standard, were 63 mm long, 12.7 mm wide, and 3 mm thick. Ten notched test specimens were used.

One-way ANOVA was performed using Statgraphics Centurion 18, Version 18.1.16, at a confidence level of 95% for the mechanical properties.

### 2.3.8. Flammability analysis

The flammability test measures how easily materials ignite, how quickly they burn, and how they react when burned. The tests were conducted for neat LLDPE and composites samples based on ASTM D635-22, in the horizontal position with a 45° flame angle. The test specimen dimensions are 125 mm long, 13 mm wide, and 3.0 mm thick. The burning rate was calculated using Equation (6), where  $V$  is the linear burning rate [ $\text{mm}\cdot\text{min}^{-1}$ ],  $L$  is the burn length [mm], and  $t$  is the time [s]. This test was done in five replicates.

$$V = \frac{60 \cdot L}{t} \quad (6)$$

## 3. Results and discussion

### 3.1. Morphology of the coir fibers

Figure 2 shows six images for each CF-100 and CF-50 sample randomly collected from their respective batches. As expected, the CF-100 is shorter than the CF-50. The CF-100 fiber appears to have suffered more damage during the milling process, resulting in a ‘crumpled’ appearance and an uneven surface. Furthermore, the CF-100 appears to have an irregular diameter and length. On the other hand, the CF-50 fiber appears to have a more regular structure, a smoother surface, and fewer imperfections than the CF-100. Milling destroys the original bundles, and the fibers degraded in length do not show the external

form of the original fiber [43]. Since CF-50 is the longest fiber, it has higher potential to produce composites with superior mechanical behavior [2] than the ones with CF-100. On the other hand, the presence of fibers with irregular contours and sharp regions may produce points of stress concentrators, which can have a negative effect on the mechanical behavior of composites. Therefore, it is expected that the difference in the morphologies between CF-50 and CF100 fibers may impact the properties of composites.

### 3.2. Effect of coir content and size on composite properties

#### 3.2.1. Density and melt flow index

Table 4 shows the comparison of densities of CF, neat LLDPE, and LLDPE/CF composites.

LLDPE/CF composites show similar experimental density values as neat LLDPE, regardless of the fiber content. This behavior contrasts with rotomolded composite literature [5, 44] data, which shows a slight increase in density of lignocellulosic composites, also expected according to the theoretical values in Table 3. For instance, López-Bañuelos *et al.* [44] reported a density of  $1.01 \text{ g}\cdot\text{cm}^{-3}$  for a linear medium-density polyethylene (LMDPE) filled with 15% agave fiber and  $0.94 \text{ g}\cdot\text{cm}^{-3}$  for neat LMDPE. Hanana *et al.* [5] reported a density of  $1.04 \text{ g}\cdot\text{cm}^{-3}$  for LLDPE filled with 20% maple fiber and  $0.93 \text{ g}\cdot\text{cm}^{-3}$  for neat LLDPE. Furthermore, as the CF content in the composite increases, the density ratio of experimental/theoretical ( $E/T$  ratio) decreases. As the CF content increases, the LLDPE/CF composites lighten, possibly due to an increase in material porosity. The polymer plastification process may generate voids and gaps during rotomolding. These voids and gaps remain in the mass until it cools, leaving a porous

**Table 4.** Density and melt flow index of LLDPE and LLDPE/CF composites [wt%].

LDPE/CF/CF-mesh	Density [ $\text{g}\cdot\text{cm}^{-3}$ ]			MFI [ $\text{g}\cdot 10 \text{ min}^{-1}$ ]
	Experimental, $E$	Theoretical <sup>a</sup> , $T$	$E/T$ ratio	
100/0/0	0.92±0.10	0.937	0.98	4.80±0.20
95/5/100	0.89±0.10	0.951	0.94	4.48±0.18
87.5/12.5/100	0.91±0.10	0.972	0.93	3.68±0.18
80/20/100	0.89±0.10	0.994	0.90	2.64±0.22
95/5/50	0.93±0.10	0.951	0.98	4.00±0.10
87.5/12.5/50	0.92±0.10	0.972	0.94	3.20±0.10
80/20/50	0.91±0.10	0.994	0.91	2.56±0.22

<sup>a</sup>Determined using density values for CF:  $1.220 \text{ g}\cdot\text{cm}^{-3}$  and LLDPE:  $0.937 \text{ g}\cdot\text{cm}^{-3}$ .

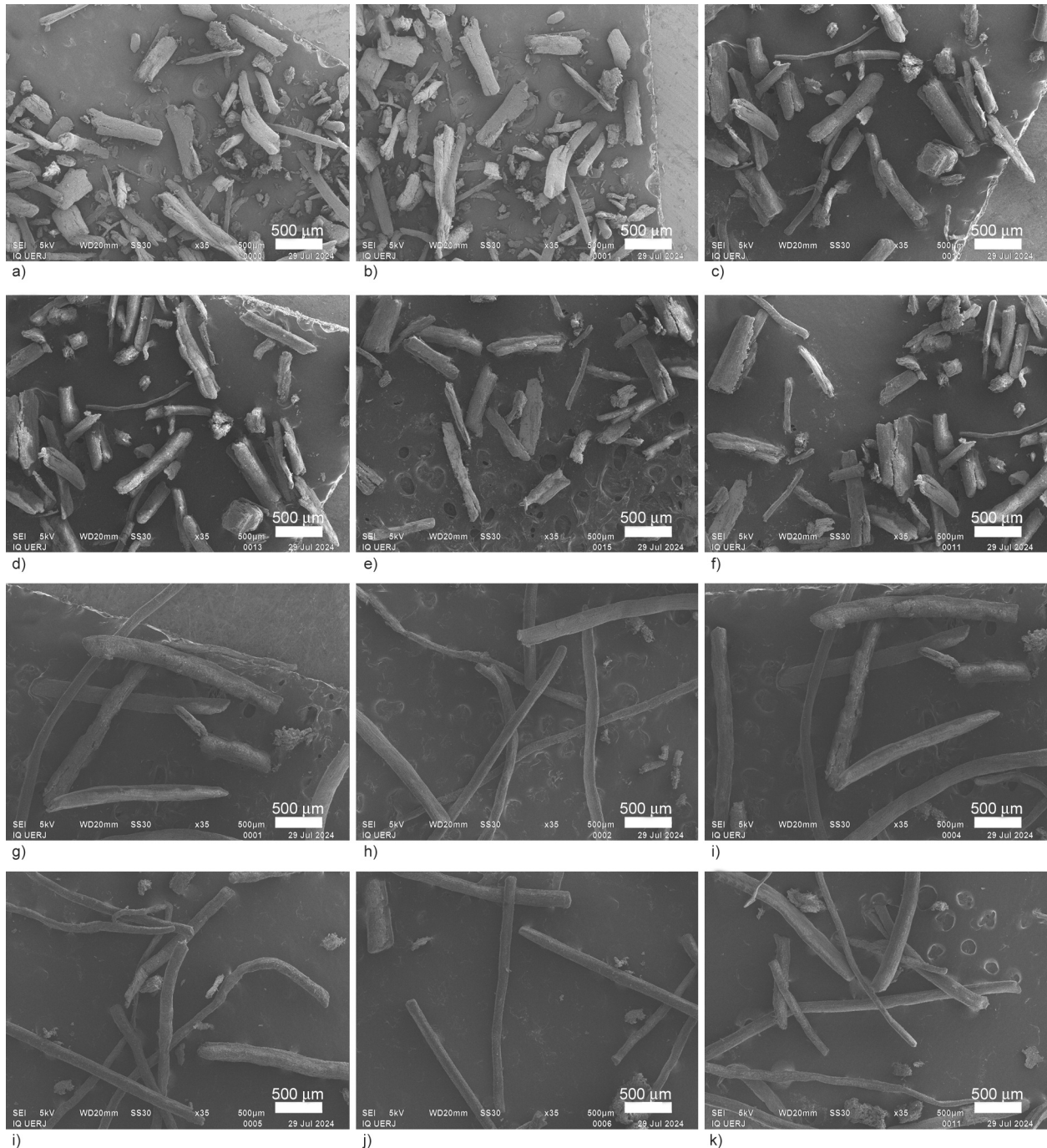


**Figure 2.** SEM images (magnification 500 µm) of CF-100 (a)–(f) and CF-50 (g)–(l) fibers.

surface for the molded part [34, 45]. Furthermore, the presence of vegetal fiber, which is a hydrophilic material, may promote bubble formation [5].

The measured *MFI* for the neat LLDPE (100/0/0) was observed to be close to the value reported by the supplier ( $5 \text{ g} \cdot 10 \text{ min}^{-1}$ ), indicating that no degradation occurred during rotomolding. In addition, increasing the amount of CF in the composite resulted in a decrease in *MFI*, regardless of the size of the fiber. The fiber acts as a barrier to polymer flow, resulting in an increase in molten mass viscosity [46,

47]. Despite the apparent lack of significant differences in *MFI* values when compared to composites with the same fiber content, the hypothesis test for paired samples was used to more specifically assess the influence of fiber size on *MFI*. This analysis rejects the null hypothesis for the comparisons of 95/5/100 and 95/5/50 ( $p$ -value = 0.00293) and 87.5/12.5/100 and 87.5/12.5/50 ( $p$ -value = 0.00293) composites, but not for the comparison of 80/20/100 and 80/20/50 ( $p$ -value = 0.5811) composites. The results show that the *MFI* decreased when CF was

added to LLDPE at a weight of 12.5% and a mesh size of 50.

### 3.2.2. Thermogravimetric analysis

Figure 3 depicts the thermal degradation behavior of neat LLDPE (100/0/0) and LLDPE/CF-100 composites. The LLDPE/CF-50 curves were not shown because their profiles are similar to those of CF-100 composites. Table 5 shows the temperatures obtained from the TGA and DTA curves.

As expected, Figure 3 and Table 5 show that neat LLDPE (100/0/0) has a single-stage process, while LLDPE/CF composites have two main degrading events. The first event is caused by the thermal degradation of CF, and the second one is caused by LLDPE. Prasad *et al.* [48] stated the thermal degradation of untreated coir fibers, evaluated by TGA at a heating rate of  $10^{\circ}\text{C}\cdot\text{min}^{-1}$  in a nitrogen atmosphere, occurred between 200 and  $380^{\circ}\text{C}$  (hemicellulose, lignin, and cellulose), which is consistent with the temperature range of the first degradation event depicted in Figure 3. Regardless of its size, the addition of CF reduces the thermal stability of the LLDPE matrix, which is to be expected given that CF has lower thermal stability than LLDPE. A report indicates that adding lignocellulosic fibers to an

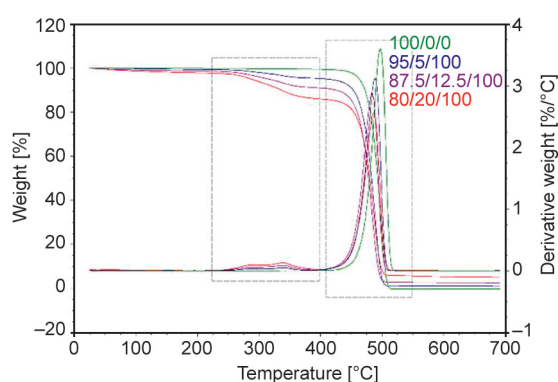


**Figure 3.** Overlay of TGA/DTG curves of neat LLDPE (100/0/0) and LLDPE/CF/CF-100 composites [wt%].

**Table 5.** Temperatures obtained from the TGA and DTA curves of neat LLDPE (100/0/0) and LLDPE/CF composites [wt%].

LDPE/CF/CF-mesh	$T_{\text{onset}}$ [°C]	$T_{\text{max1}}$ [°C]	$T_{\text{max2}}$ [°C]
100/0/0	479	–	497
95/5/100	289	340	488
87.5/12.5/100	279	339	484
80/20/100	282	340	486
95/5/50	302	351	494
87.5/12.5/50	284	342	490
80/20/50	287	347	492

LLDPE matrix reduces its thermal stability [48]. However, because the  $T_{\text{onset}}$  values of LLDPE/CF composites are significantly higher than the typical operating temperatures of LLDPE-based rotomolded products, their lower thermal stability does not impede their use. No TGA results were found in the literature for rotomolded LLDPE/coir fiber composites that would allow a better comparison with those from this study.

### 3.2.3. Crystallinity degree measurement

Table 6 displays the enthalpies ( $\Delta H$ ), temperature of crystallization ( $T_c$ ), and crystallinity degree ( $\chi_c$ ) of both neat LLDPE (100/0/0) and LLDPE/CF composites. In general, the difference of  $\chi_c$  between the first and second heating cycles is minimal (approximately 2% on average), indicating that all samples reach their maximum degree of crystallization during rotomolding.

In addition, the  $\chi_c$  of neat LLDPE (44% in the second heating) is similar to the values determined by Li *et al.* [41] (40%) and Gupta and Ramkumar [2] (41%). Regarding the effect of CF on  $\chi_c$ , it is evident that CF does not act as a nucleating agent as  $T_c$  values of composites are not higher than the value of LLDPE. In fact, the addition of CF produces the opposite behavior, specifically a slight decrease in  $T_c$ . In addition,

**Table 6.** Enthalpies and crystallinity of neat LLDPE (100/0/0) and LLDPE/CF/CF-mesh composites [wt%].

LDPE/CF/CF-mesh	$T_m$ 1 <sup>st</sup> [°C]	$\Delta H$ 1 <sup>st</sup> [J·kg <sup>-1</sup> ]	$\chi_c$ 1 <sup>st</sup> [%]	$T_c$ [°C]	$T_m$ 2 <sup>nd</sup> [°C]	$\Delta H$ 2 <sup>nd</sup> [J·kg <sup>-1</sup> ]	$\chi_c$ 2 <sup>nd</sup> [%]
100/0/0	131	136.6	47	114	127	128.9	44
95/5/100	130	127.0	46	111	125	122.4	44
87.5/12.5/100	130	127.4	50	115	126	124.6	49
80/20/100	130	108.8	46	112	126	104.1	44
95/5/50	129	124.5	45	111	126	121.9	44
87.5/12.5/50	130	123.6	48	111	126	117.7	46
80/20/50	130	118.7	51	111	126	112.8	48

there appears to be no correlation between  $\chi_c$  and the amount of CF in the composites. The average of  $\chi_c$  for the first heating cycle for all composites is 48% (standard deviation of 2%) whereas the value for LLDPE is 47%. As a result, the presence of CF does not inhibit LLDPE crystallization during the cooling phase of rotomolding. Choudhury *et al.* [29] showed that the crystallinity of polyethylene decreased with the incorporation of short coconut coir fibers (40  $\mu\text{m}$ ) due to the reduction in the structural regularity and packing capacity of the polymer chains in the presence of the fibers, which probably also occurred in this study. Gupta and Ramkumar [2] found a gradually increasing the degree of crystallinity (41, 45, 46, 46, 48%,) with increasing the amount of coir fiber (0, 3, 5, 7 and 10 wt%, respectively) added in LLDPE due to increasing the nucleation arrangement.

### 3.2.4. Water absorption

The water absorption assessment is an important property for composites filled with lignocellulosic fibers because the excessive water content can cause issues such as dimensional instability and premature degradation [22]. Figure 4 shows the water absorption against time for all composites.

Due to its hydrophobic nature, neat-LLDPE (100/0/0) practically exhibits no weight gain during continuous water immersion. Conversely, an increase in coir content leads to an increase in water absorption over time. Robledo-Ortiz *et al.* [22] observed this behavior and stated that water absorption is influenced by the degree of interaction between the hydrophobic polymer and hydrophilic filler. The authors of [22]

reported a water absorption of around 17% for 1008 h of test for the composite with 20 and 30 wt% of coir fiber, which is lower than our results. The presence of cavities, gaps, and other imperfections throughout the material facilitates water diffusion, thereby speeding up the process. Further, the increased fiber length and volume in the composite also contributes to increased water absorption [32]. Figure 4 demonstrates that LLDPE composites filled with 12.5 and 20 wt% of CF-50 absorb water more quickly than composites filled with CF-100 with the same fiber content. This finding suggests that, despite having a similar density to LLDPE/CF-100 (as discussed in the Section 3.2.1), the LLDPE/CF-50 composites may have a structure with larger cavities and gaps. Another factor that can contribute to the increase in water absorption is the size of the fiber, since CF-50 is longer than CF-100, as shown in Figure 2.

### 3.2.5. Mechanical properties

All properties have ANOVA p-values less than 0.05, indicating a statistically significant difference between the samples. In order to identify which samples are significantly different from each other, mean plots were generated for impact resistance (Figure 5), modulus of elasticity and flexural modulus (Figure 6), and tensile and flexural strengths (Figure 7). In this analysis, a pair of intervals that do not overlap indicates a statistically significant difference between the samples at a confidence level of 0.05.

Figure 5 shows that all composites become weaker as the CF content increases, regardless of fiber size. Only the 95/5/50 composite has the same impact resistance as the neat LLDPE. The 87.5/12.5/100,

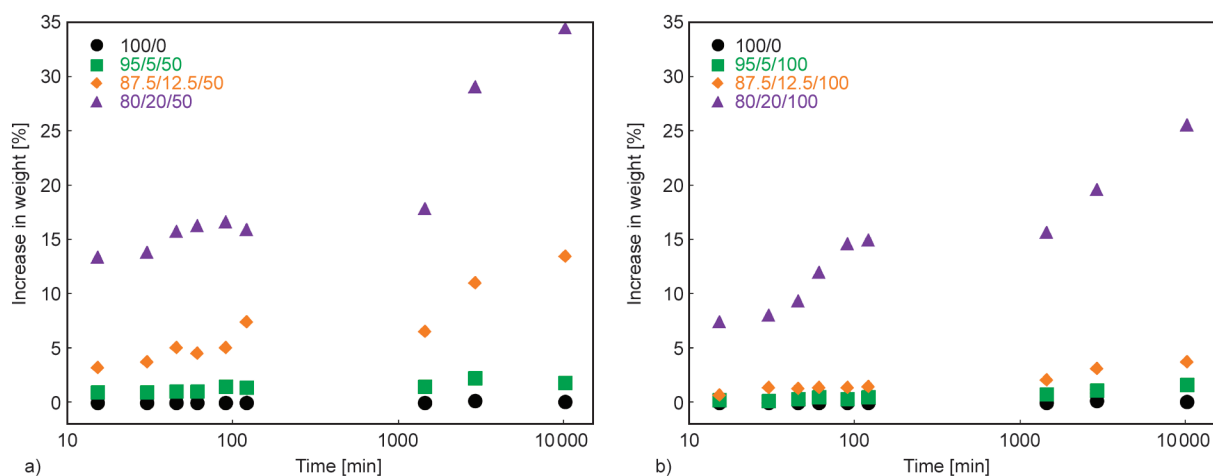


**Figure 4.** Water absorption test: comparison of weight increase *versus* time for neat-LLDPE (100/0/0) and LLDPE composites filled with a) CF-50 and b) CF-100.

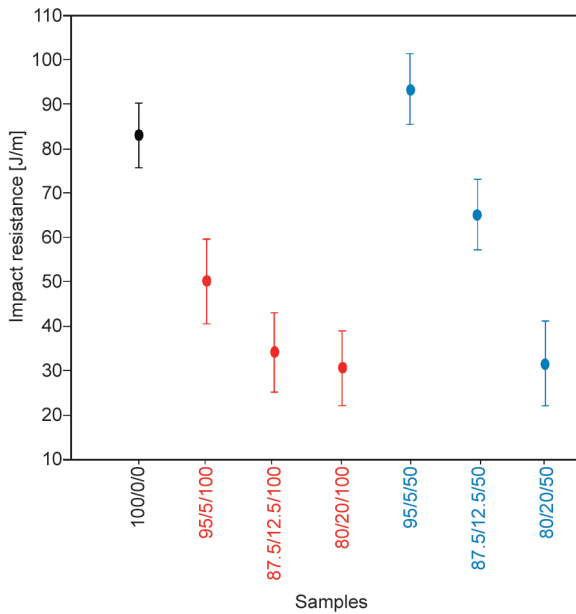


**Figure 5.** Impact resistance of neat LLDPE (100/0/0) and LLDPE/CF/CF-mesh composites [wt%].

80/20/100, and 80/20/50 composites all exhibit the same lowest impact resistance due to the overlap of their respective mean intervals. Adding CF-50 at a low concentration appears to have a less negative effect on impact resistance. Robledo-Ortíz *et al.* [22] also reported a decrease in impact resistance of the LLDPE composites with 20 and 30 wt% of coir fiber, regardless of if the fiber was treated or not. According to the authors, factors that affect the impact resistance are interaction between fiber-matrix, porosity, and fiber agglomeration. In this study, the main factor that contributes to reducing impact

resistance is fiber size and morphology. As previously discussed, the CF-100 is shorter fiber with more imperfections than CF50 (Figure 2). Therefore, the likelihood of the CF-100 having more stress concentrator points is higher than that of the CF-50, which facilitates fracture propagation.

The mechanical properties shown in Figure 6 and Figure 7 follow the same pattern as the impact resistance pattern in Figure 5. As the amount of CF increases, the property modulus of elasticity, flexural modulus, tensile strength, and flexural strength all go down. The flexural modulus values (Figure 6b) were practically the same for the composites with CF-100 and CF-50 mesh, regardless of the fiber content and quantity. The tensile modulus for the composites with CF-100 fiber showed anomalous behavior, mainly for the 87.5/12.5/100 composite, indicating that some random factor affected the cube production. In terms of CF-50 fiber, the 95/5/50 and 87.5/12.5/50 composites had similar and higher modulus values than the 80/20/50 composite. This shows that adding more fiber makes the property worse (Figure 6a). Similar behavior is found for tensile and flexural strengths, shown in Figure 6. In fact, the tensile properties of composites with CF-50 appear to have an inverse correlation with the increase in fiber content, whereas the composites with CF-100 fiber do not exhibit this behavior.

As previously discussed in Section 3.1, it was expected to observe the positive impact of the length of CF fiber and the amount on the mechanical properties of

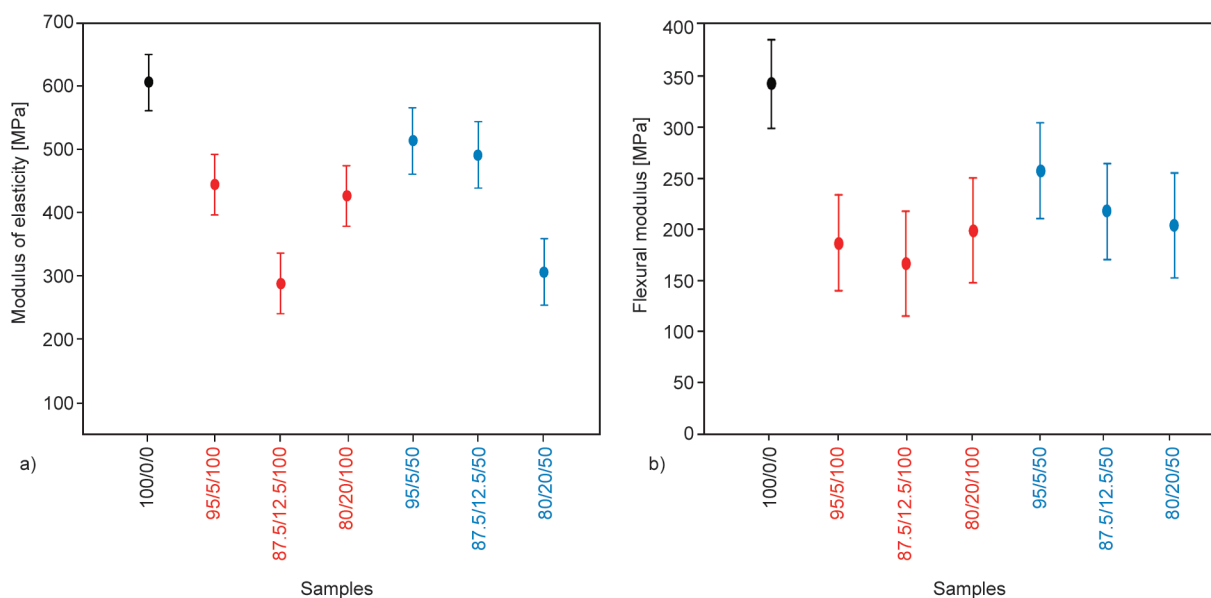


**Figure 6.** Modulus of elasticity (a) and flexural modulus (b) of neat LLDPE (100/0/0) and LLDPE/CF/CF-mesh composites [wt%].

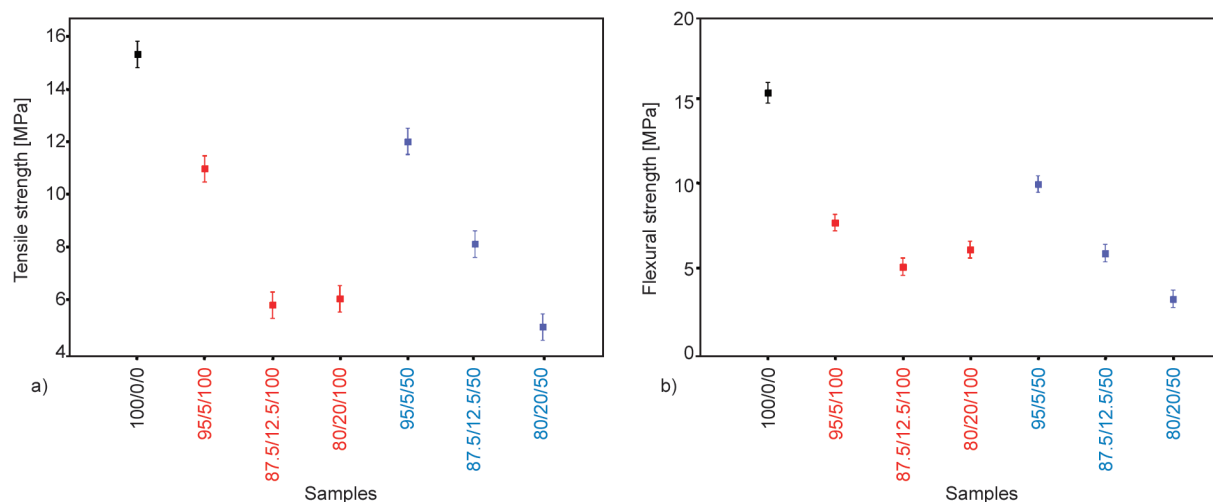


**Figure 7.** Tensile strength (a) and flexural strength (b) of neat LLDPE (100/0/0) and LLDPE/CF/CF-mesh composites [wt%].

the composite [2, 49–51]. However, these correlations were not observed in this study. Furthermore, the more fragmented nature of CF-100 (Figure 2), characterized by irregular contours and crumples, contributed to the occurrence of “side effects”, which in turn made this anomalous behavior more evident. As a result, the deterioration of mechanical properties observed in the study can be attributed mainly to the poor adhesion between coir fibers and LLDPE, the presence of voids in the matrix, which reduce the fiber size effect on the properties, and the irregular (damaged) morphology of the fibers. Abhilash and Singaravelu [52] reported a similar deterioration of mechanical properties, despite having previously treated the coir fiber with NaOH. Robledo-Ortiz *et al.* [22] showed that the incorporation of untreated fiber into the matrix decreased flexural strength from 21.4 MPa (neat PE) to 10.4 MPa with the addition of 20 wt% coconut fiber, and to 8 MPa with 30 wt%. In contrast, Gupta and Ramkumar [2] observed an increase in elastic modulus (around 10%) and impact resistance (around 15%) with increasing fiber content up to 7 wt%, which contradicts our findings. Comparing this study with Gupta and Ramkumar [2], it is found that there are significant differences in the LLDPE grade used in both studies. For example, the elastic modulus of neat LLDPE used in the present work is 607 MPa, whereas Gupta and Ramkumar [2] reported a value of 255 MPa.

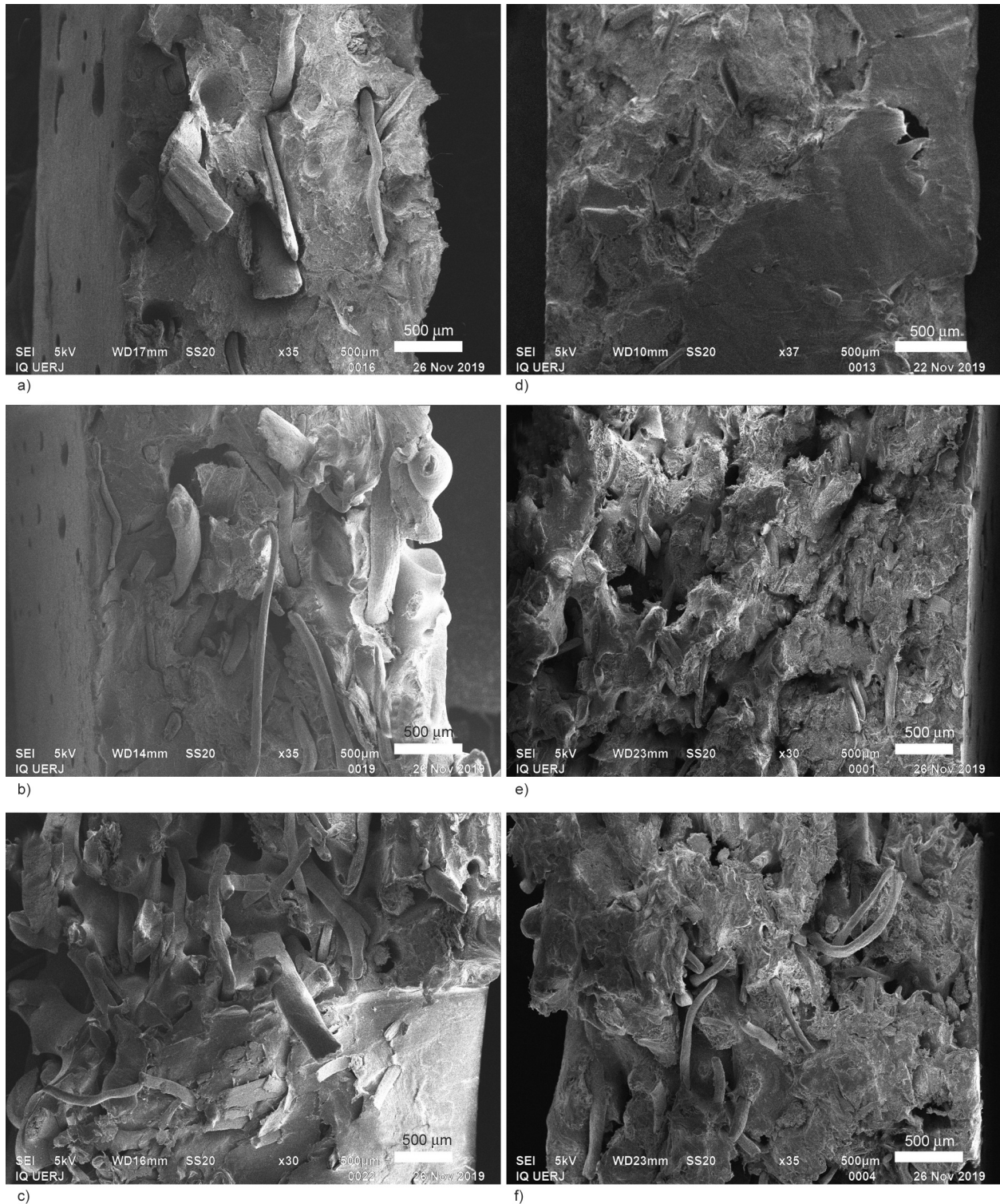
### 3.2.6. Morphology of the LLDPE/CF composites

Figure 8 depicts SEM images of the impact test surface of LLDPE/CF composites.

As expected, more fibers become visible as the fiber content increases, but no agglomerates are visible. The voids surrounding the fibers clearly indicate a lack of interaction between coir fiber and LLDPE. López-Bañuelos *et al.* [44] and Hanana *et al.* [5] also reported a similar lack of interaction between lignocellulosic fiber and LLDPE. This incompatibility is a result of LLDPE's hydrophobicity and CF's hydrophilicity [53]. Moreover, all samples showed some voids and appear to have coir fibers oriented in the transverse direction of the thickness. According to the literature [34, 54], the presence of voids can be attributed to the presence of residual moisture in the CF fibers or to insufficient sintering densification of the LLDPE. Nevertheless, neither of these two causes could be responsible for the observed voids in the samples, as the void shapes seen in the micrographs are not characteristic of bubbles. In fact, the rotational process lacks sufficient shear to produce a well-mixed fiber and matrix composite, particularly when the two components are incompatible. The fiber and LLDPE then fail to adhere, resulting in microvoids that expand during an impact test. In addition, the presence of microvoids reinforces the lower  $E/T$  density ratios, as previously discussed.

### 3.2.7. Flammability analysis

The flammability test revealed that all samples dripped. Furthermore, the neat-LLDPE (100/0/0) sample deformed, whereas the LLDPE/CF composites maintained their shape. This behavior suggests that CF plays a structural role in burning composites. Figure 9 displays a comparison of the linear burning



**Figure 8.** SEM images (magnification 500 μm) of cryofractured surface of LLDPE/CF/CF-mesh [wt%]: a) 95/5/50, b) 87.5/12.5/50, c) 80/20/50, d) 95/5/100, e) 87.5/12.5/100, f) 80/20/100.

rates of the neat LLDPE (100/0/0) and the LLDPE/CF composites.

The linear burning rate of neat LLDPE (100/0/0) is  $65 \text{ mm} \cdot \text{min}^{-1}$ , which is higher than the literature values reported for HDPE ( $20 \text{ mm} \cdot \text{min}^{-1}$ ) [55] and waste plastic bag ( $15 \text{ mm} \cdot \text{min}^{-1}$ ) [56]. When considering how CF affects the burning rate, it is clear

that only the fiber size has a significant impact on the flammability behavior. For example, the linear burning rate for LLDPE composites with CF-100 fibers goes up a lot, but it doesn't change at all for CF-50 fibers. The increased surface area of smaller fibers (CF-100) is responsible for this result. According to da Sylva Rocha *et al.* [55], the addition

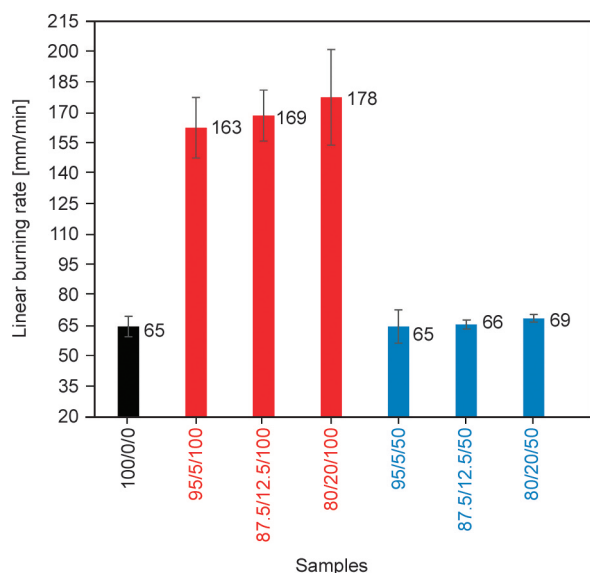


**Figure 9.** Linear burning rate of neat LLDPE (100/0/0) and LLDPE/CF/CF-mesh composites [wt%].

of lignocellulosic fibers leads to an increase in the burning rate of HDPE composites. This paper compared the flammability results with various lignocellulosic fibers, but it did not verify the relationship between flammability and fiber size. In the study by Umemura *et al.* [57], the polypropylene-based wood-plastic composites burn faster than neat polymers. In this study, wood is in the form of wood flour, a material with a high surface area. Studies [58, 59] on the effect of the non-renewable fiber lengths on the flammability of composites have been carried out, and differences have been observed. For instance, Savas *et al.* [58] observed no effect of carbon fiber length on flammability. Ghazzawi *et al.* [59] suggest that short fiber (usually not larger than 5–10 mm) contributes to the barrier effects during combustion if combined with a high carbonization polymer matrix. The size of the flame retardant strongly influences its efficiency [60].

### 3.3. Effect of coupling agent type on composite properties

#### 3.3.1. Density, melt flow index and water absorption

The densities and Melt Flow Index (*MFI*) values for 95/5/100, 95/5/100/MAPE, 95/5/100/CaSt, and 95/5/100/MgSt composites are shown in Table 7.

The comparison of density data, shown in Table 7, reveals that there is no significant difference observed among the values. This finding suggests that the type of additive does not contribute to the reduction of porosity in the 95/5/100/0 composite. In addition, adding CaSt and MgSt additives has the opposite effect, since 95/5/100/CaSt and 95/5/100/MgSt composites showed a higher water absorption over time compared to 95/5/100/0 and 95/5/100/MAPE (Figure 10). This implies that the use of stearates in the LLDPE/coir fiber composites likely results in the formation of bigger pores. This behavior was not expected since it was reported in the literature [22, 29] that the addition of a compatibilizing agent in LLDPE and coconut fiber composites would cause a decrease in water absorption. According to Robledo-Ortiz *et al.* [22], surface treatment with MAPE decreased the water affinity of polyethylene composites with 20 and 30 wt% coconut fiber, leading to water absorption values lower than 20 wt% in the composites. The improvement of fiber-matrix interfacial bonding reduces water accumulation in interfacial gaps or voids, preventing water from entering the fibers [29]. Kulikov and co-workers [33, 61] found that glycerol monostearate, calcium stearate, and zinc stearate decrease the melt viscosity and elasticity of LLDPE, leading to faster densification and bubble removal. The two stearate types used in this investigation do not decrease the porosity or viscosity (Table 7 and Figure 10). One reason that can

**Table 7.** Density and melt flow index of 95/5/100, 95/5/100/MAPE, 95/5/100/CaSt, and 95/5/100/MgSt composites [wt%].

LDPE/CF/CF-mesh/additive	Density [g·cm <sup>-3</sup> ]			<i>MFI</i> [g·10 min <sup>-1</sup> ]
	Experimental, <i>E</i>	Theoretical <sup>a</sup> , <i>T</i>	<i>E/T</i>	
95/5/100/0	0.89±0.10	0.951	0.94	4.48±0.18
95/5/100/MAPE	0.93±0.10	0.951	0.98	4.93±0.23
95/5/100/CaSt	0.91±0.10	0.953	0.95	4.32±0.18
95/5/100/MgSt	0.91±0.10	0.952	0.96	4.40±0.40

<sup>a</sup>Determined using the density of CF: 1.220 g·cm<sup>-3</sup> and LLDPE: 0.937 g·cm<sup>-3</sup>.

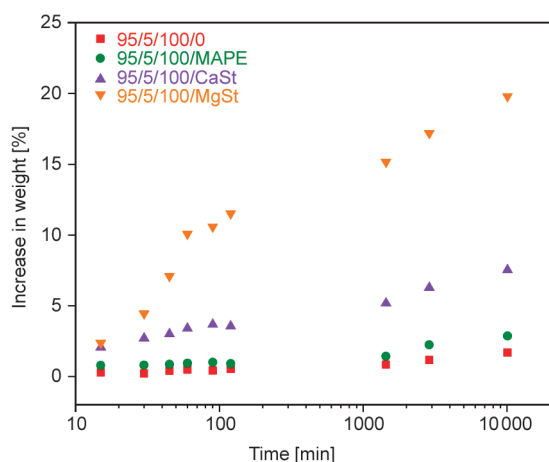


**Figure 10.** Water absorption test: comparison of increase in weight vs. time of 95/5/100/0, 95/5/100/MAPE, 95/5/100/CaSt, and 95/5/100/MgSt composites [wt%].

contribute to this contradictory behavior is that all ingredients in the formulation were manually mixed before the rotomolding process. Additionally, the lower density of LLDPE ( $0.937 \text{ g}\cdot\text{cm}^{-3}$ ) compared to CaSt ( $1.08 \text{ g}\cdot\text{cm}^{-3}$ ) and MgSt ( $1.03 \text{ g}\cdot\text{cm}^{-3}$ ) contributed to the segregation of the additives in the composites. The amount of MAPE used in this study can be insufficient to promote a reduction in porosity in the 95/5/100/MAPE composite. In this case, the hypothesis of segregation is not considered due to the proximity in density between MAPE ( $0.905 \text{ g}\cdot\text{cm}^{-3}$ ) and LLDPE ( $0.937 \text{ g}\cdot\text{cm}^{-3}$ ).

### 3.3.2. Mechanical property – modulus of elasticity

Figure 11 shows the results of modulus of elasticity of tensile test for 95/5/100/0, 95/5/100/MAPE, 95/5/100/CaSt, and 95/5/100/MgSt composites.

The elastic modulus of the 95/5/100/MAPE composite exhibits a similar magnitude as that of the 95/5/100/0 composite. The present finding diverges from the results reported by Hanana *et al.* [5] and Cisneros-López *et al.* [23], which stated an increase in this particular property with the presence of MAPE. The absence of favorable findings in the modulus of elasticity for 95/5/100/MAPE may be attributed to the ineffective contribution of MAPE as a coupling agent in this system. Consequently, coir fibers and LLDPE have poor adhesion and matrix voids. Additionally, it is clear that the modulus of elasticity of the 95/5/100/CaSt and 95/5/100/MgSt is significantly lower than that of the 95/5/100/0 composite. Since no increase in the *MFI* values is observed (Table 6),

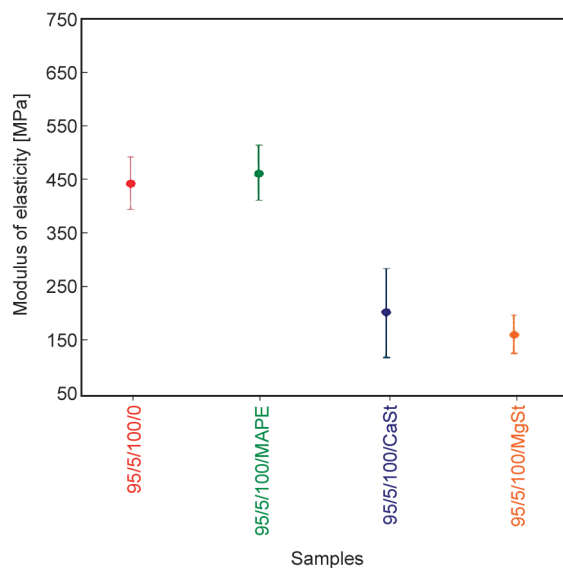


**Figure 11.** Modulus of elasticity of LLDPE/CF/CF-mesh/additive composites: 95/5/100/0, 95/5/100/MAPE, 95/5/100/CaSt, and 95/5/100/MgSt [wt%].

one cannot justify the reduction of modulus because of the plasticizer effect of CaSt or MgSt. The rotomolding process commonly uses stearates as internal release agents. According to Yeetsorn *et al.* [62] higher concentrations of these substances have a negative effect on the mechanical properties of the final products. So, a plausible cause for a decrease in modulus is the inadequate dispersion of the additives within the matrix, resulting in regions with higher contents and contributing to mechanical property deterioration. As a result, the aforementioned findings indicate that incorporating the components of the composites without prior mixing, such as in an extruder, is not the optimal approach for manufacturing rotomolding products.

## 4. Conclusions

The influence of the incorporation of coconut fiber (CF) in the LLDPE matrix on rotomolded composite properties was observed when compared to the pure polymer. In general, composites containing CF-50 perform better than those with CF-100. This result was attributed to the fact that CF-100 is more fragmented and irregular than CF-50. Further, increasing the CF content causes a decrease in the mechanical properties. This is due to the ineffective adhesion between coir fibers and LLDPE, as well as the presence of voids in the matrix. The results showed that using MAPE, CaSt, or MgSt as additives did not contribute to reducing the porosity of the composites. Moreover, MAPE performed better than calcium and

magnesium stearates in the elastic modulus of the 95/5/100/0 composite, although no reduction in the porosity was observed. Our future work will be carried out using prior extrusion of the composite to seek greater interaction between the components and a smaller number of bubbles.

Thermogravimetric analysis indicated a shift in degradation temperatures to lower temperatures with the addition of fiber to LLDPE, with values around 280 °C for compositions with 12.5 and 20 wt% fiber, regardless of the mesh, and values around 290–300 °C for composites with 5 wt% of fiber (50 and 100 mesh). Neat LLDPE began to degrade at 479 °C. All composites with CF-50 showed similar flammability behavior to the neat LLDPE.

In general, a composite with 5 wt% of CF-50 or CF-100 has promising potential for hollow rotomolded parts. The presence of ethylene maleic anhydride copolymer (MAPE) in the composite with 5 wt% of CF-100 also proved promising. The result is quite interesting from an environmental aspect, as it is a more renewable material and is obtained with less energy consumption, since an extruder was not used for its prior mixing. Large-scale rotomolded parts can be produced with this composite and can be used in equipment casings and storage boxes, which are generally large parts for agricultural grains, such as cotton, peanuts, soybeans, beans etc. Rotomolding allows the production of hermetic and seamless parts, in addition to the parts being customizable. Furthermore, products with lower technical requirements, such as ornaments and large decorative objects, can be produced with composites with a higher percentage of fiber (10 and 20 wt%), which results in a more renewable product in comparison to using neat LLDPE.

### Acknowledgements

The authors thank the *Coordenação de Aperfeiçoamento de Pessoal de Nível Superior* (CAPES) for the grant awarded to Lumirca Del Valle Espinoza León. The authors also thank *Fundação de Amparo à Pesquisa do Estado do Rio de Janeiro* (FAPERJ) and *Conselho Nacional de Desenvolvimento Científico e Tecnológico* (CNPq).

### References

- [1] Aniśko J., Barczewski M., Mietliński P., Piasecki A., Szulc J.: Valorization of disposable polylactide (PLA) cups by rotational molding technology: The influence of pre-processing grinding and thermal treatment. *Polymer Testing*, **107**, 107481 (2022).  
<https://doi.org/10.1016/j.polymertesting.2022.107481>
- [2] Gupta N., Ramkumar P. L.: Effect of coir content on mechanical and thermal properties of LLDPE/coir blend processed by rotational molding. *Sādhanā*, **46**, 40 (2021).  
<https://doi.org/10.1007/s12046-021-01566-8>
- [3] del Valle Espinoza León L., Escocio V. A., Visconte L. L. Y., Jandorno J. C. Jr., Pacheco E. B. A. V.: Rotomolding and polyethylene composites with rotomolded lignocellulosic materials: A review. *Journal of Reinforced Plastics and Composites*, **39**, 459–472 (2020).  
<https://doi.org/10.1177/0731684420916529>
- [4] Alemán D. N. C., McCourt M., Kearns M. P., Martin P. J., Butterfield J.: The development of thermoplastic fibre-based reinforcements for the rotational moulding process. in ‘Proceedings of the 21<sup>st</sup> International Esaform Conference On Material Forming: ESAFORM 2018, Palermo, Italy’ 120002 (2018).  
<https://doi.org/10.1063/1.5034970>
- [5] Hanana F. E., Desiré C. Y., Rodrigue D.: Morphology and mechanical properties of maple reinforced LLDPE produced by rotational moulding: Effect of fibre content and surface treatment. *Polymers and Polymer Composites*, **26**, 299–308 (2018).  
<https://doi.org/10.1177/096739111802600404>
- [6] Höfler G., Lin R. J., Jayaraman K.: Rotational moulding and mechanical characterisation of halloysite reinforced polyethylenes. *Journal of Polymer Research*, **25**, 32–142 (2018).  
<https://doi.org/10.1007/s10965-018-1525-3>
- [7] Girijappa Y. G. T., Rangappa S. M., Parameswaranpillai J., Siengchin S.: Natural fibers as sustainable and renewable resource for development of eco-friendly composites: A comprehensive review. *Frontiers in Materials, Section Polymeric and Composite Materials*, **6**, 226 (2019).  
<https://doi.org/10.3389/fmats.2019.00226>
- [8] Karimah A., Ridho M. R., Munawar S. S., Adi D. S., Ismadi, Damayanti R., Subiyanto B., Fatriasari W., Fudholi A.: A review on natural fibers for development of eco-friendly bio-composite: Characteristics, and utilizations. *Journal of Materials Research and Technology*, **13**, 2442–2458 (2021).  
<https://doi.org/10.1016/j.jmrt.2021.06.014>

- [9] Prasad V., Vijayakumar A. A., Jose T., George S. C.: A comprehensive review of sustainability in natural-fiber-reinforced polymers. *Sustainability*, **16**, 1223 (2024). <https://doi.org/10.3390/su16031223>
- [10] Mujtaba M., Fraceto L. F., Fazeli M., Mukherjee S., Savassa S. M., de Medeiros G. A., do Espírito Santo Pereira A. E. S., Mancini S. D., Lipponen J., Vilaplana F.: Lignocellulosic biomass from agricultural waste to the circular economy: A review with focus on biofuels, biocomposites and bioplastics. *Journal of Cleaner Production*, **402**, 136815 (2023). <https://doi.org/10.1016/j.jclepro.2023.136815>
- [11] Malviya R. K., Singh R. K., Purohit R., Sinha R.: Natural fibre reinforced composite materials: Environmentally better life cycle assessment – A case study. *Materials Today: Proceedings*, **26**, 3157–3160 (2020). <https://doi.org/10.1016/j.matpr.2020.02.651>
- [12] Mansor M. R., Mastura M. T., Sapuan S. M., Zainudin A. Z.: The environmental impact of natural fiber composites through life cycle assessment analysis in ‘Durability and life prediction in biocomposites, fibre-reinforced composites and hybrid composites’ (eds.: Jawaid M., Thariq M., Saba N.) Woodhead, Sawston, 257–285 (2019). <https://doi.org/10.1016/B978-0-08-102290-0.00011-8>
- [13] Ead A. S., Appel R., Alex N., Ayranci C., Carey J. P.: Life cycle analysis for green composites: A review of literature including considerations for local and global agricultural use. *Journal of Engineered Fibers and Fabrics*, **16**, 1–22 (2012). <https://doi.org/10.1177/15589250211026940>
- [14] Broeren M. L. M., Dellaert S. N. C., Cok B., Patel M. K., Worrell E., Shen L.: Life cycle assessment of sisal fibre – Exploring how local practices can influence environmental performance. *Journal of Cleaner Production*, **149**, 818–827 (2017). <https://doi.org/10.1016/j.jclepro.2017.02.073>
- [15] Hejna A., Barczewski M., Andrzejewski J., Kosmela P., Piasecki A., Szostak M., Kuang T.: Rotational molding of linear low-density polyethylene composites filled with wheat bran. *Polymers*, **12**, 1004 (2020). <https://doi.org/10.3390/polym12051004>
- [16] Andrzejewski J., Krawczak A., Wesoly K., Szostak M.: Rotational molding of biocomposites with addition of buckwheat husk filler. Structure-property correlation assessment for materials based on polyethylene (PE) and poly(lactic acid) PLA. *Composites Part B: Engineering*, **202**, 108410 (2020). <https://doi.org/10.1016/j.compositesb.2020.108410>
- [17] Hanana F. E., Rodrigue D.: Effect of particle size, fiber content, and surface treatment on the mechanical properties of maple-reinforced LLDPE produced by rotational molding. *Polymers and Polymer Composites*, **29**, 343–353 (2021). <https://doi.org/10.1177/0967391120916602>
- [18] Saraiva A. B., Pacheco E. B. A. V., Gomes G. M., Visconte L. L. Y., Bernardo C. A., Simões C. L., Soares A. G.: Comparative lifecycle assessment of mango packaging made from A polyethylene/natural fiber-composite and from cardboard material. *Journal of Cleaner Production*, **139**, 1168–1180 (2016). <https://doi.org/10.1016/j.jclepro.2016.08.135>
- [19] Abhilash S. S., Singaravelu D. L.: Effect of fiber content on mechanical and morphological properties of bamboo fiber-reinforced linear low-density polyethylene processed by rotational molding. *Transactions of the Indian Institute of Metals*, **73**, 1549–1554 (2020). <https://doi.org/10.1007/s12666-020-01922-y>
- [20] Zhao X., Li R. K. Y., Bai S-L.: Mechanical properties of sisal fiber reinforced high density polyethylene composites: Effect of fiber content, interfacial compatibilization, and manufacturing process. *Composites Part A: Applied Science and Manufacturing*, **65**, 169–174 (2014). <https://doi.org/10.1016/j.compositesa.2014.06.017>
- [21] Marin D., Chiarello L. M., Wiggers V. R., de Oliveira A. D., Botton V.: Effect of coupling agents on properties of vegetable fiber polymeric composites: Review. *Polímeros: Ciência e Tecnologia*, **33**, e20230012 (2023). <https://doi.org/10.1590/0104-1428.20220118>
- [22] Robledo-Ortíz J. R., González-López M. E., Rodrigue D., Gutiérrez-Ruiz J. F., Prezas-Lara F., Pérez-Fonseca A. A.: Improving the compatibility and mechanical properties of natural fibers/green polyethylene biocomposites produced by rotational molding. *Journal of Polymers and the Environment*, **28**, 1040–1049 (2020). <https://doi.org/10.1007/s10924-020-01667-1>
- [23] Cisneros-López E. O., González-López M. E., Pérez-Fonseca A. A., González-Núñez R., Rodrigue D., Robledo-Ortíz J. R.: Effect of fiber content and surface treatment on the mechanical properties of natural fiber composites produced by rotomolding. *Composite Interfaces*, **24**, 35–53 (2017). <https://doi.org/10.1080/09276440.2016.1184556>
- [24] Samanth M., Bhat K. S.: Conventional and unconventional chemical treatment methods of natural fibres for sustainable biocomposites. *Sustainable Chemistry for Climate Action*, **3**, 100034 (2023). <https://doi.org/10.1016/j.scca.2023.100034>
- [25] Boman A., Miguel M., Andersson I., Slunge D.: The effect of information about hazardous chemicals in consumer products on behaviour – A systematic review. *Science of the Total Environment*, **947**, 174774 (2024). <https://doi.org/10.1016/j.scitotenv.2024.174774>
- [26] Cisneros-López E. O., Pérez-Fonseca A. A., Fuentes-Talavera F. J., Anzaldo J., González-Núñez R., Rodrigue D., Robledo-Ortíz J. R.: Rotomolded polyethylene-agave fiber composites: Effect of fiber surface treatment on the mechanical properties. *Polymer Engineering & Science*, **56**, 856–865 (2016). <https://doi.org/10.1002/pen.24314>

- [27] Pereira P. H. F., Rosa M. F., Cioffi M. O. H., Benini K. C. C. C., Milanese A. C., Voorwald H. J. C., Mulinari D. R.: Vegetal fibers in polymeric composites: A review. *Polímeros*, **25**, 9–22 (2015).  
<https://doi.org/10.1590/0104-1428.1722>
- [28] Kramer D. G., Rocha B. G., Pereira M. C. S., Souza R. S. D., Alves C. R., Cavalcanti G. B. Jr., Oliveira H., Quina M. J., Gando-Ferreira L., Lachumananandasivam R.: Determination of the biosorption of cd(II) by coconut fiber. *Journal of Agricultural Science and Technology*, **4**, 291–298 (2014).
- [29] Choudhury A., Kumar S., Adhikari B.: Recycled milk pouch and virgin low-density polyethylene/linear low-density polyethylene based coir fiber composites. *Journal of Applied Polymer Science*, **106**, 775–785 (2007).  
<https://doi.org/10.1002/app.26522>
- [30] Escócio V. A., Pacheco E. B. A. V. P., Souza A. M. F., Brígida M. A. C. S., Soares A. G., Visconte L. L. Y.: Study of natural fibers from waste from sponge gourd, peach palm tree and papaya pseudstem. *International Journal of Agriculture and Environmental Research*, **3**, 11–24 (2017).
- [31] Elfaleh I., Abbassi F., Habibi M., Ahmad F., Guedri M., Nasri M., Garnier C.: A comprehensive review of natural fibers and their composites: An eco-friendly alternative to conventional materials. *Results in Engineering*, **19**, 101271 (2023).  
<https://doi.org/10.1016/j.rineng.2023.101271>
- [32] Hasan K. M. F., Horváth P. G., Bak M., Alpár T.: A state-of-the-art review on coir fiber-reinforced biocomposites. *RSC Advances*, **11**, 10548–10571 (2021).  
<https://doi.org/10.1039/d1ra00231g>
- [33] Kulikov O., Hornung K., Wagner M.: Novel processing additives for rotational molding of polyethylene. *International Polymer Processing*, **24**, 452–462 (2009).  
<https://doi.org/10.3139/217.2296>
- [34] Crawford R. J., Throne J. L.: *Rotational molding technology*. William Andrew, New York (2002).
- [35] Mitchell P. E.: *Tool and manufacturing engineers handbooks*, Vol. 8. Plastic art manufacturing rotational molding. Society of Manufacturing Engineers, Southfield (1996).
- [36] Wang B., Panigrahi S., Tabil L., Crerar W.: Pre-treatment of flax fibers for use in rotationally molded biocomposites. *Journal of Reinforced Plastics and Composites*, **26**, 447–463 (2007).  
<https://doi.org/10.1177/0731684406072526>
- [37] Nugent P.: Plastic processing: Rotational moulding. in ‘Applied plastics engineering handbook’ (ed.: Myer K.) Elsevier, New York, 311–332 (2011).
- [38] Crawford R. J., Spence A. G., Cramez M. C., Oliveira M. J.: Mould pressure control in rotational moulding. *Proceedings of the Institution of Mechanical Engineers Part B*, **218**, 1683–1693 (2004).  
<https://doi.org/10.1177/095440540421801204>
- [39] Linowski J. W., Liu N-I., Jonas J.: The effect of density and temperature on the hydroxyl proton chemical shift in liquid ethanol. *Journal of Magnetic Resonance*, **23**, 455–460 (1976).  
[https://doi.org/10.1016/0022-2364\(76\)90278-X](https://doi.org/10.1016/0022-2364(76)90278-X)
- [40] Khanam P. N., AlMaadeed M. A. A.: Processing and characterization of polyethylene-based composites. *Advanced Manufacturing: Polymer & Composites Science*, **1**, 63–79 (2015).  
<https://doi.org/10.1179/2055035915Y.0000000002>
- [41] Li D., Zhou L., Zhou L., Wang X., He L., Yang X.: Effect of crystallinity of polyethylene with different densities on breakdown strength and conductance property. *Materials*, **12**, 1746 (2019).  
<https://doi.org/10.3390/ma12111746>
- [42] Ramkumar P. L., Gupta N., Sangani V.: Experimental investigation on underlying mechanism of LLDPE based rotationally molded biocomposites. *Journal of Natural Fibers*, **20**, 2156022 (2023).  
<https://doi.org/10.1080/15440478.2022.2156022>
- [43] Csiszár E., Fekete E., Tóth A., Bandi É., Koczka B., Sajó I.: Effect of particle size on the surface properties and morphology of ground flax. *Carbohydrate Polymers*, **94**, 927–933 (2013).  
<https://doi.org/10.1016/j.carbpol.2013.02.026>
- [44] López-Bañuelos R. H., Moscoso F. J., Ortega-Gudiño P., Mendizabal E., Rodrigue D., González-Núñez R.: Rotational molding of polyethylene composites based on agave fibers. *Polymer Engineering & Science*, **52**, 2489–2497 (2012).  
<https://doi.org/10.1002/pen.23168>
- [45] Ogila K. O., Shao M., Yang W., Tan J.: Rotational molding: A review of the models and materials. *Express Polymer Letters*, **11**, 778–798 (2017).  
<https://doi.org/10.3144/expresspolymlett.2017.75>
- [46] Escócio V. A., Pacheco E. B. A. V., Furtado A. M., Cavalcante P. A., Visconte L. L. Y.: Use of spongegourd (*Luffa cylindrica*) agro-residue as filler for renewable high density polyethylene: Development and characterization of composites. *International Journal of Materials Engineering*, **12**, 151–176 (2014).
- [47] Ramkumar P. L., Kulkarni D. M., Abhijit V. V. R., Cherukumudi A.: Investigation of melt flow index and impact strength of foamed LLDPE for rotational moulding process. *Procedia Materials Science*, **6**, 361–367 (2014).  
<https://doi.org/10.1016/j.mspro.2014.07.046>
- [48] Prasad N., Agarwal V. K., Sinha S.: Thermal degradation of coir fiber reinforced low-density polyethylene composites. *Science and Engineering of Composite Materials*, **25**, 363–372 (2018).  
<https://doi.org/10.1515/secm-2015-0422>

- [49] Lapique F., Meakin P., Feder J., Jøssang T.: Relationships between microstructure, fracture–surface morphology, and mechanical properties in ethylene and propylene polymers and copolymers. *Journal of Applied Polymer Science*, **77**, 2370–2382 (2000).  
[https://doi.org/10.1002/1097-4628\(20000912\)77:11<2370::aid-app5>3.0.co;2-6](https://doi.org/10.1002/1097-4628(20000912)77:11<2370::aid-app5>3.0.co;2-6)
- [50] Nestore O., Kajaks J., Vancovicha I., Reihmane S.: Physical and mechanical properties of composites based on a linear low-density polyethylene (LLDPE) and natural fiber waste. *Mechanics of Composite Materials*, **48**, 619–628 (2013).  
<https://doi.org/10.1007/s11029-013-9306-x>
- [51] Debabeche N., Kribaa O., Boussehel H., Guerira B., Jawaid M., Fouad H., Azeem M. A.: Effect of fiber surface treatment on the mechanical, morphological, and dynamic mechanical properties of palm petiole fiber/LLDPE composites. *Biomass Conversion and Biorefinery*, **14**, 20699–20712 (2023).  
<https://doi.org/10.1007/s13399-023-04197-7>
- [52] Abhilash S. S., Singaravelu D. L.: A comparative study of mechanical, dynamic mechanical and morphological characterization of tampico and coir fibre-reinforced LLDPE processed by rotational moulding. *Journal of Industrial Textiles*, **51**, 285S–310S (2022).  
<https://doi.org/10.1177/1528083720929363>
- [53] Saba N., Tahir P. M., Jawaid M.: A review on potentiality of nano filler/natural fiber filled polymer hybrid composites. *Polymers*, **6**, 2247–2273 (2014).  
<https://doi.org/10.3390/polym6082247>
- [54] Thakur V. K., Thakur M. K., Gupta R. K.: Review: Raw natural fiber–based polymer composites. *International Journal of Polymer Analysis and Characterization*, **19**, 256–271 (2014).  
<https://doi.org/10.1080/1023666X.2014.880016>
- [55] da Silva Rocha J., Escócio V. A., Visconte L. L. Y., Pacheco É. B. A. V.: Thermal and flammability properties of polyethylene composites with fibers to replace natural wood. *Journal of Reinforced Plastics and Composites*, **40**, 726–740 (2021).  
<https://doi.org/10.1177/07316844211002895>
- [56] Dhawan R., Bisht B. M. S., Kumar R., Kumari S., Dhawan S. K.: Recycling of plastic waste into tiles with reduced flammability and improved tensile strength. *Process Safety and Environmental Protection*, **124**, 299–307 (2019).  
<https://doi.org/10.1016/j.psep.2019.02.018>
- [57] Umemura T., Arao Y., Nakamura S., Tomita Y., Tanaka T.: Synergy effects of wood flour and fire retardants in flammability of wood-plastic composites. *Energy Procedia*, **56**, 48–56 (2014).  
<https://doi.org/10.1016/j.egypro.2014.07.130>
- [58] Savas L. A., Mutlu A., Dike A. S., Tayfun U., Dogan M.: Effect of carbon fiber amount and length on flame retardant and mechanical properties of intumescent polypropylene composites. *Journal of Composite Materials*, **52**, 519–530 (2018).  
<https://doi.org/10.1177/0021998317710319>
- [59] Ghazzawi Y. M., Osorio A. F., Heitzmann M. T.: The effect of fibre length and fibre type on the fire performance of thermoplastic composites: The behaviour of polycarbonate as an example of a charring matrix. *Construction and Building Materials*, **234**, 117889 (2020).  
<https://doi.org/10.1016/j.conbuildmat.2019.117889>
- [60] Tomiak F., Schartel B., Wolf M., Drummer D.: Particle size related effects of multi-component flame-retardant systems in poly(butadiene terephthalate). *Polymers*, **12**, 1315 (2020).  
<https://doi.org/10.3390/polym12061315>
- [61] Kulikov O., Hornung K., Wagner M.: Control of nano-scale structuring and reinforcement in rotational molding of polyethylene. *Macromolecular Symposia*, **296**, 324–335 (2010).  
<https://doi.org/10.1002/masy.201051045>
- [62] Yeetsorn R., Prissanaroon-Ouajai W., Boonpanaid C., Onyu K., Simon L.: Rotomoulding release agent preparation for auto part fabrications. *Materials Today: Proceedings*, **52**, 2365–2371 (2022).  
<https://doi.org/10.1016/j.matpr.2021.10.100>